

## Effect of grain size on domain structures, dielectric and thermal depoling of Nd-substituted bismuth titanate ceramics

Giuseppe Viola, Kok Boon Chong, Mirva Eriksson, Zhijian Shen, Jiangtao Zeng, Qingrui Yin, Yanmei Kan, Peiling Wang, Huanpo Ning, Hongtao Zhang, Michael E. Fitzpatrick, Michael J. Reece, and Haixue Yan

Citation: *Applied Physics Letters* **103**, 182903 (2013); doi: 10.1063/1.4827537

View online: <http://dx.doi.org/10.1063/1.4827537>

View Table of Contents: <http://scitation.aip.org/content/aip/journal/apl/103/18?ver=pdfcov>

Published by the AIP Publishing

### Articles you may be interested in

Study of domain structure of poled (K,Na)NbO<sub>3</sub> ceramics

J. Appl. Phys. **113**, 204107 (2013); 10.1063/1.4807919

De-aging of Fe-doped lead-zirconate-titanate ceramics by electric field cycling: 180°- vs. non-180° domain wall processes

J. Appl. Phys. **112**, 034103 (2012); 10.1063/1.4739721

Ferroelectric domain wall pinning at a bicrystal grain boundary in bismuth ferrite

Appl. Phys. Lett. **93**, 142901 (2008); 10.1063/1.2993327

Effect of substitution of Nd<sup>3+</sup> for Bi<sup>3+</sup> on the dielectric properties and structures of SrBi<sub>2- $\chi$</sub> Nd $\chi$ Nb<sub>2</sub>O<sub>9</sub> bismuth layer-structured ceramics

J. Appl. Phys. **101**, 084102 (2007); 10.1063/1.2724818

Microstructural, ferroelectric, and dielectric properties of Bi<sub>3.15</sub>Nd<sub>0.85</sub>Ti<sub>3</sub>O<sub>12</sub> ceramics

J. Appl. Phys. **98**, 094101 (2005); 10.1063/1.2103418

You don't  
still use this  
cell phone



or this computer



Why are you  
still using an  
AFM designed  
in the 80's?



**It is time to upgrade your AFM**

Minimum \$20,000 trade-in discount  
for purchases before August 31st

**Asylum Research is today's  
technology leader in AFM**

[dropmyoldAFM@oxinst.com](mailto:dropmyoldAFM@oxinst.com)



*The Business of Science®*

# Effect of grain size on domain structures, dielectric and thermal depoling of Nd-substituted bismuth titanate ceramics

Giuseppe Viola,<sup>1</sup> Kok Boon Chong,<sup>2</sup> Mirva Eriksson,<sup>3</sup> Zhijian Shen,<sup>3</sup> Jiangtao Zeng,<sup>4</sup> Qingrui Yin,<sup>4</sup> Yanmei Kan,<sup>4</sup> Peiling Wang,<sup>4</sup> Huanpo Ning,<sup>1</sup> Hongtao Zhang,<sup>1,5</sup> Michael E. Fitzpatrick,<sup>2</sup> Michael J. Reece,<sup>1,6</sup> and Haixue Yan<sup>1,6,a)</sup>

<sup>1</sup>*School of Engineering and Materials Science, Queen Mary University of London, London E1 4NS, United Kingdom*

<sup>2</sup>*Materials Engineering, The Open University, Walton Hall, MK7 6AA Milton Keynes, United Kingdom*

<sup>3</sup>*Arrhenius Laboratory, Department of Materials and Environmental Chemistry, Stockholm University, S-10691 Stockholm, Sweden*

<sup>4</sup>*Shanghai Institute of Ceramics, Chinese Academy of Sciences, Shanghai 200050, People's Republic of China*

<sup>5</sup>*Department of Materials, University of Oxford, Oxford OX1 3PH, United Kingdom*

<sup>6</sup>*Nanoforce Technology Ltd, London E1 4NS, United Kingdom*

(Received 10 June 2013; accepted 14 October 2013; published online 30 October 2013)

The microscopic origin of the grain size effects on the dielectric, piezoelectric, and thermal depoling properties of Aurivillius phase  $\text{Bi}_{3.15}\text{Nd}_{0.85}\text{Ti}_3\text{O}_{12}$  was investigated. Using atomic force microscopy, domain walls were observed in micrometer grain size ceramics, but gradually disappeared with reducing grain size and were not found in ceramics with 90 nm grain size. In strain-electric field butterfly loops, the strain decreased with decreasing grain size indicating a decreasing contribution of non-180° domain walls switching to the strain. Lattice distortion  $(a-b)/b$  decreased with decreasing grain size. The thermal depoling resistance decreased with decreasing grain size, due to increasing internal mechanical stresses. © 2013 AIP Publishing LLC. [<http://dx.doi.org/10.1063/1.4827537>]

Grain size effects in ferroelectric materials is important for fundamental research and industrial applications.<sup>1,2</sup> When the grain dimension is below a critical size, ferroelectricity disappears, affecting the performance of devices.<sup>2,3</sup> There have been many studies of grain size effects on ferroelectric domain structures in bulk perovskite ferroelectric ceramics.<sup>4–8</sup> In lead-zirconate-titanate (PZT) ceramics, the non-180° ferroelectric domain size decreases with the square root of the grain size when grain size is from 0.2 to 10  $\mu\text{m}$ . The domain size of PZT decreases more quickly for grains below 0.2  $\mu\text{m}$ .<sup>4</sup> In  $\text{BaTiO}_3$  ceramics, ferroelectric domain walls were observed in grains with size larger than 500 nm.<sup>6</sup> Single domain and single grain structure was observed in  $\text{BaTiO}_3$  ceramics when grain size is less than 400 nanometers.<sup>8</sup> In  $(\text{NaK})_{0.5}\text{NbO}_3$  ferroelectric ceramics, ferroelectric domain size decreases linearly with grain size in the range of 0.2 to 1  $\mu\text{m}$ . The minimum domain width is 30 nm in 200 nm sized grain.<sup>7</sup>

Aurivillius phase ferroelectrics are good candidates for non-volatile ferroelectric random-access memory (FRAM) because of their fatigue-free properties.<sup>9</sup> However, there have been limited reports on grain size effects in Aurivillius phase ferroelectrics.<sup>10–12</sup> Their crystal structures are considerably different from perovskite structure. The difference may result in different grain size effects. Aurivillius phase formula is  $(\text{Bi}_2\text{O}_2)^{2+}(\text{A}_{m-1}\text{B}_m\text{O}_{3m+1})^{2-}$ , where A-site element and B-site element are cuboctahedral coordination and octahedral coordination, respectively. The  $m$  is the number of octahedral layers.<sup>13–15</sup> The even-layer ( $m=2$ ,  $\text{Bi}_3\text{NbTiO}_9$ ;  $m=4$   $\text{CaBi}_4\text{Ti}_4\text{O}_{15}$ ) Aurivillius phase compounds are orthorhombic with space group  $A2_1am$ . Their spontaneous

polarization is along the  $a$ -axis. The odd-layer Aurivillius phase compound ( $m=3$ ,  $\text{Bi}_4\text{Ti}_3\text{O}_{12}$ ) is monoclinic with space group  $Pc$ . The spontaneous polarization is within  $a$ - $c$  plane with the major polarization along the  $a$ -axis.<sup>15–18</sup>

Neodymium-substituted bismuth titanate ( $\text{Bi}_{3.15}\text{Nd}_{0.85}\text{Ti}_3\text{O}_{12}$ ) (BNT) is a three layered Aurivillius phase ferroelectric material. BNT thin film is interesting for FRAM application due to its significantly enhanced remanent polarization and fatigue resistance.<sup>19,20</sup> In the present work the microscopic origin of the grain size effects on dielectric, piezoelectric, and thermal depoling properties of BNT was investigated.

BNT ceramics with different grain size were prepared using a spark plasma sintering furnace at 750 °C, 850 °C, and 1000 °C, hereafter referred to as BNT750, BNT850, and BNT1000, respectively.<sup>10</sup> The density of the BNT ceramics was measured by the Archimedes immersion method. The domain structures of BNT ceramics sintered at different temperatures were examined by an atomic force microscope (AFM) (SPA 400, SPI3800N, Seiko Inc. Japan) in piezoresponse mode.<sup>21</sup> A Ti/Pt-coated Si cantilever with 2- $\mu\text{m}$ -thickness and 90- $\mu\text{m}$ -length (Micro Masch, NSC12-B) was used. The used spring constant was 14 N/m and resonance frequency was 315 kHz. The applied static force to the tip was set to 7 nN. Domain structures were characterized under an applied ac voltage with amplitude  $V_{ac}=14$  V and frequency  $f=10$  kHz. The high resolution powder diffraction beamline 6-ID-D at Advanced Photon Source, Argonne National Laboratory (USA) was employed for the precise lattice parameter characterization. Tests were performed on the crushed ceramics at room temperature. The dielectric constant and loss at different frequencies were measured using an impedance analyser (4294 A, Agilent, CA) at room temperature. The ferroelectric

<sup>a)</sup> Author to whom correspondence should be addressed. Electronic mail: [h.x.yan@qmul.ac.uk](mailto:h.x.yan@qmul.ac.uk)

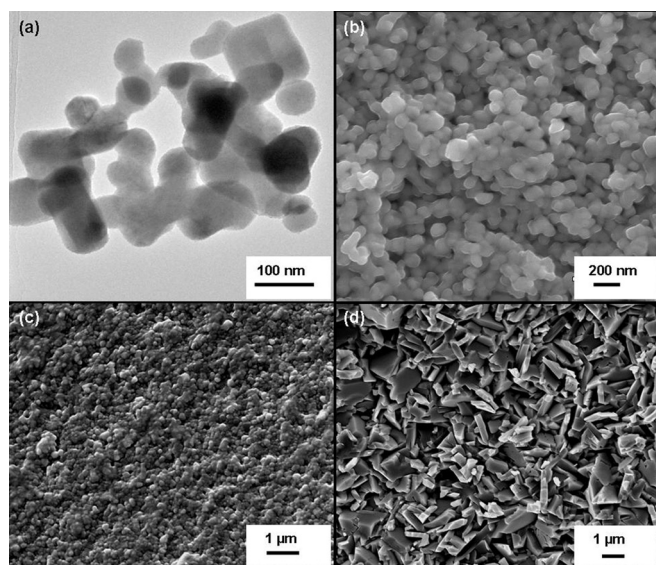


FIG. 1. TEM image of (a) BNT powder produced by hydrolysis method and SEM images of fracture surface of ceramics: (b) BNT750; (c) BNT850; and (d) BNT1000.

strain-electric field hysteresis loops were obtained at room temperature using a capacitance nanosensor device (NPL, Teddington, UK).<sup>22,23</sup> For piezoelectric constant measurements the samples were poled under DC conditions with an electric field of 10 kV/mm for 15 min in silicone oil at room temperature. The piezoelectric constant ( $d_{33}$ ) was characterized using a piezo- $d_{33}$  meter (ZJ-3B, Institute of Acoustics, Academia Sinica). Thermal depoling properties were investigated by measuring the variation of the piezoelectric constant  $d_{33}$  at room temperature after repeated heat treatments at incrementally higher annealing temperatures where the poled specimens were kept for 2 h and then naturally cooled at room temperature. The silver electrodes of poled samples were removed using acetone before thermal depoling measurement.

The densities of the BNT ceramics were 97.5%, 98.0%, and 99.6% for BNT750, BNT850, BNT1000, respectively. Figure 1(a) shows a TEM micrograph of the nanopowder which exhibits equiaxed shape and forms agglomerates. Figures 1(b)–1(d) display the SEM micrographs of the fracture surface of the three ceramics. BNT750 and BNT850 ceramics (Figs. 1(b) and 1(c)) show equiaxed grain morphology, while in BNT1000 (Fig. 1(d)) the grains become platelet-like. The estimated average grain size was  $90 \pm 10$  nm and  $160 \pm 20$  nm for BNT750 and BNT850, and  $2011 \pm 30$  nm in length and  $307 \pm 30$  nm in thickness for BNT1000.<sup>10</sup> Figure 2 shows the topographic (left column) and piezoelectric force microscopy (PFM) image (right column) of BNT samples sintered at different temperatures. All the measurements were performed on polished surfaces. The grain boundaries were not clear except for BNT1000 (Fig. 2(c)). There were no domain structures apparent in the topographic images. In the PFM images, the bright areas correspond to polarization vectors pointing out of the sample, while dark regions (arrow marked) reflect a polarization pointing into the sample. Areas with grey contrast correspond to in-plane or zero polarization. For BNT750 (Fig. 2(a)), no contrast could be seen in the PFM image, which indicates that either the piezoresponse or the domain size was too small to be detected or there were no

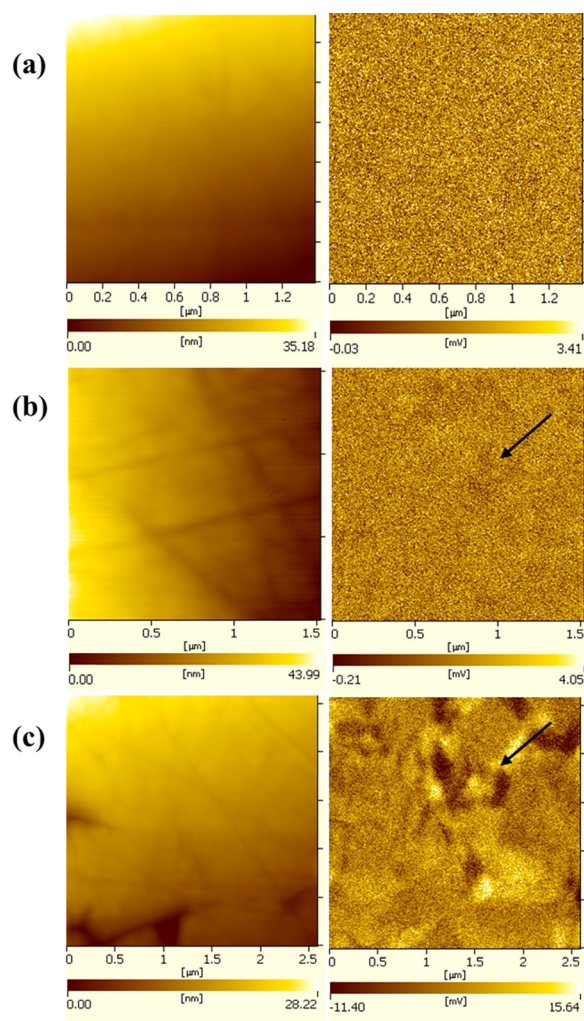


FIG. 2. Topographic images (left) and PFM images (right): (a) BNT750; (b) BNT850; and (c) BNT1000.

domain walls in grains. For BNT850 (Fig. 2(b)), some areas were slightly darker, representing evidence for domain structure. In contrast, the domain structure was very clear for BNT1000 (Fig. 2(c)). The domain size ranges approximately from 100 nm to 250 nm. According to previous studies on BaTiO<sub>3</sub> ceramics, when the grain size is below a critical value of (300–500 nm),<sup>6,24</sup> the domain walls disappear and each grain tends to assume single domain configuration. There were clear domain walls in BNT1000, but not in BNT750 as shown in Fig. 2.

In BNT the largest spontaneous polarization is along the  $a$ -axis.<sup>16–18</sup> Figure 3 shows the lattice distortion ( $a-b$ )/ $b$  of BNT ceramics with different grain sizes. The lattice parameter measurements were performed on the crushed ceramics at room temperature and the results suggest that BNT exhibited orthorhombic structure. The lattice distortion decreased with reducing grain size. This is consistent with previous studies in bismuth titanate ceramics.<sup>11,12</sup> In ferroelectric/ferroelastic systems, non-180° domains appear across the paraelectric-ferroelectric phase transition to minimize electrical and mechanical internal energy. In BNT1000, the internal mechanical stress due to lattice distortion was minimized via domain wall formation (Fig. 2(c)). In BNT750, the lattice distortion was relatively low so that the induced internal mechanical stress was not sufficient to nucleate domain walls, as



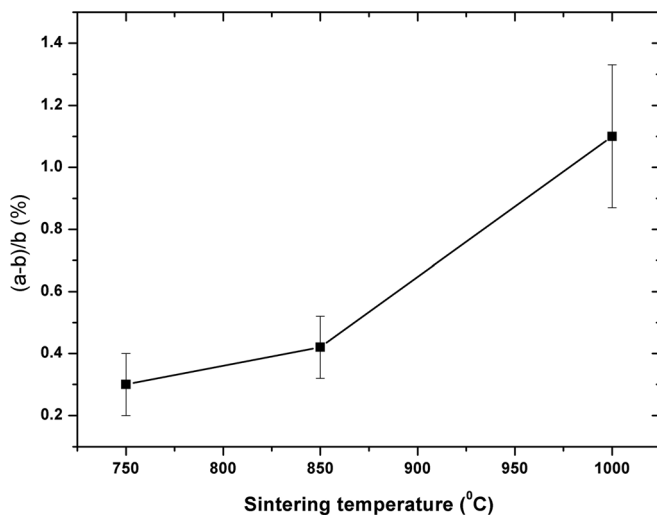


FIG. 3. Lattice distortion  $(a-b)/b$  vs. sintering temperature for BNT ceramics.

evidenced by the fact that domain walls were not observed in BNT750 (Fig. 2(a)). The internal stresses in BNT750 are expected to be higher than that in BNT1000, because in the former, the internal stresses developed during cooling through  $T_c$  could not be reduced by the formation of non-180° domain walls as evidenced by its single domain single grain structure (Fig. 2(a)).

Figure 4 shows the frequency dependence of the dielectric permittivity and dielectric loss for BNT ceramics with different grain size. The dielectric permittivity increased with decreasing grain size (Fig. 4) in agreement with the reported dielectric measurements for bismuth titanate ceramics.<sup>12</sup> There has been an intensive debate on the grain size dependence of the dielectric permittivity in barium titanate, and different models have been proposed over the past 60 years (see Ref. 24 for a succinct chronological review), but a clear understanding has not been achieved yet.<sup>25,26</sup> In this instance, the higher dielectric permittivity of BNT750 seems to be related to the higher internal mechanical stresses linked with single domain single grain structure as previously modeled.<sup>27</sup> The higher loss of BNT1000 can be attributed to the extrinsic contribution produced by the movement of the ferroelectric domain walls. This was not the case for

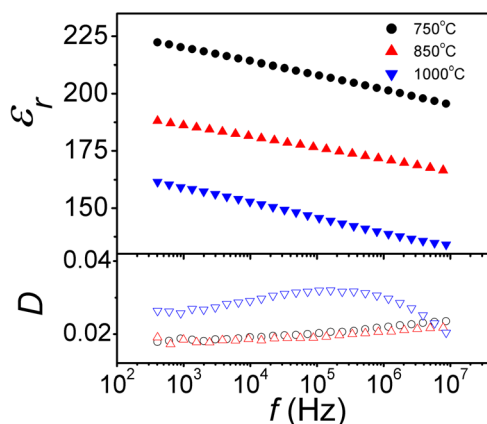


FIG. 4. Frequency dependent of dielectric permittivity and losses of BNT ceramics.

BNT750 and BNT850 because they had few or no domain walls.

Figure 5 shows the strain-electric field loops (S-E) of BNT ceramics with different grain size. The strain change in BNT750 was very small (Fig. 5(a)). Despite the large measurement background noise, the S-E loops of BNT850 and BNT1000 showed the typical butterfly shape of ferroelectric materials (Figs. 5(b) and 5(c)). The higher strain change of BNT1000 is consistent with its clear domain wall structure (Fig. 2(c)) and larger lattice distortion  $(a-b)/b$  (Fig. 3).

Figure 6 shows the effect of grain size on thermal depoling of BNT ceramics. The initial  $d_{33}$  of the ceramics with fine grain size was lower than that of the ceramics with larger grain size. This can be attributed to the fact that fine grained BNT ceramics have larger coercive field, which is related to the freezing effect in fine grained ceramics with higher stresses.<sup>10</sup> The Curie point,  $T_c$ , are  $358 \pm 5$ ,  $374 \pm 5$ ,

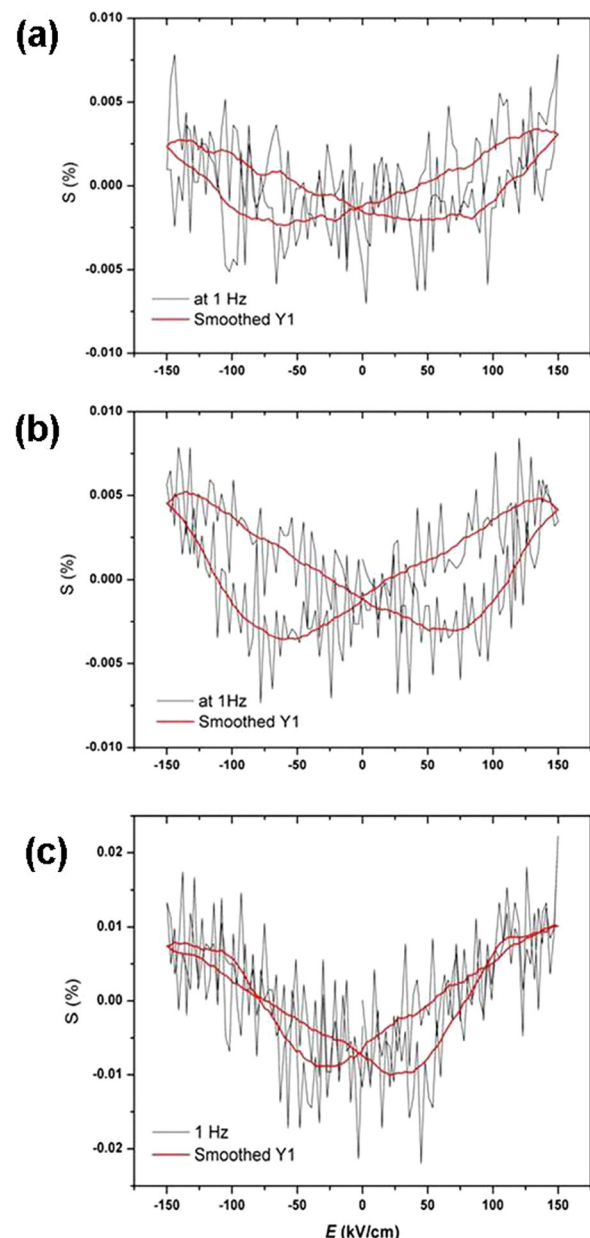


FIG. 5. Strain-electric field loops of BNT ceramics: (a) BNT750, (b) BNT850, and (c) BNT1000.

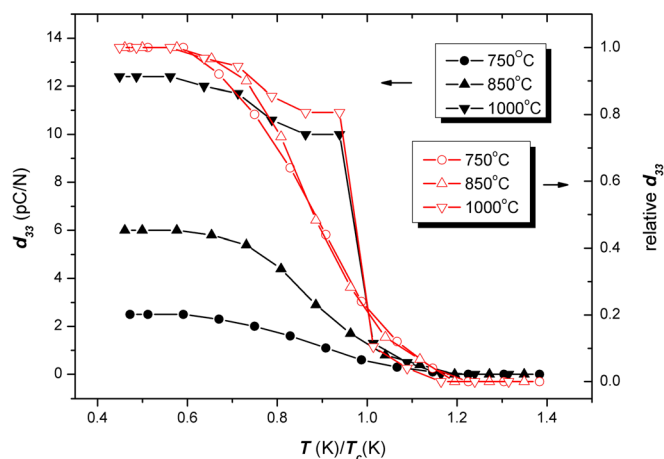


FIG. 6. Thermal depoling of BNT ceramics.

$391 \pm 5^\circ\text{C}$  for BNT750, BNT850, and BNT1000, respectively.<sup>10</sup> This can be regarded as a consequence of the fact that internal stresses tend to favor the stabilization of the paraelectric phase by suppressing the spontaneous deformation and spontaneous polarization, resulting in a lower Curie point  $T_c$ .<sup>28</sup> The  $d_{33}$  of all ceramics were thermally stable when the annealing temperature was below  $0.6T_c$ . When the annealing temperature is higher than  $0.6T_c$ , the  $d_{33}$  of ceramics with smaller grain sizes is less thermally stable than that of ceramics with larger grain sizes, which can be attributed to the higher stresses in ceramics with smaller grain size.

In summary, evidence of grain size effects on lattice distortion, domain structure, dielectric, piezoelectric, and thermal depoling properties of Aurivillius phase ferroelectric  $\text{Bi}_{3.15}\text{Nd}_{0.85}\text{Ti}_3\text{O}_{12}$  are reported. Orthorhombic distortion reduced with decreasing grain size. Ferroelectric domain walls were clearly detected in coarse-grained samples, while they were not visible in 90 nm nanograined ceramics. This is attributed to the fact that the mechanical strain produced by the ferroelectric lattice distortion in nanograined ceramics is not sufficient to nucleate the stress relieving domain walls. The higher dielectric permittivity of 90 nm grain size ceramic was attributed to the higher stresses in its single domain single grain structure. With decreasing grain size, the thermal depoling resistance decreased due to increasing internal mechanical stresses.

The authors would like to thanks Dr D. Robinson at Advanced Photon Source, Argonne National Laboratory,

USA, for the help in the high resolution powder diffraction. M.E.F. is supported by a grant through The Open University from The Lloyd's Register Educational Trust, an independent charity working to achieve advances in transportation, science, engineering, and technology education, training and research worldwide for the benefit of all.

- <sup>1</sup>V. Hornebecq, C. Huber, M. Maglione, M. Antonietti, and C. Elissalde, *Adv. Funct. Mater.* **14**, 899 (2004).
- <sup>2</sup>N. A. Spaldin, *Science* **304**, 1606 (2004).
- <sup>3</sup>J. F. Scott, *Science* **315**, 954 (2007).
- <sup>4</sup>W. Cao and C. Randall, *J. Phys. Chem. Solids* **57**, 1499 (1996).
- <sup>5</sup>T. M. Shaw, S. Trolier-McKinstry, and P. C. McIntyre, *Annu. Rev. Mater. Sci.* **30**, 263 (2000).
- <sup>6</sup>Z. Zhao, V. Buscaglia, M. Viviani, M. T. Buscaglia, L. Mitoseriu, A. Testino, M. Nygren, M. Johnsson, and P. Nanni, *Phys. Rev. B* **70**, 024107 (2004).
- <sup>7</sup>M. Eriksson, H. Yan, G. Viola, H. Ning, D. Gruner, M. Nygren, M. J. Reece, and Z. Shen, *J. Am. Ceram. Soc.* **94**(10), 3391 (2011).
- <sup>8</sup>G. Arlt, D. Hennings, and G. de With, *J. Appl. Phys.* **58**, 1619 (1985).
- <sup>9</sup>B. H. Park, B. S. Kang, S. D. Bu, T. W. Noh, J. Lee, and W. Jo, *Nature* **401**, 682 (1999).
- <sup>10</sup>H. Zhang, H. Yan, H. Ning, M. J. Reece, M. Eriksson, Z. Shen, Y. Kan, and P. Wang, *Nanotechnology* **20**, 385708 (2009).
- <sup>11</sup>K. Zhu, M. Zhang, Y. Deng, J. Zhou, and Z. Yin, *Solid State Commun.* **145**, 456 (2008).
- <sup>12</sup>H. Chen, B. Shen, J. Xu, and J. Zhai, *J. Alloys Compd.* **551**, 92 (2013).
- <sup>13</sup>V. A. Isupov, *Ferroelectrics* **189**, 211 (1996).
- <sup>14</sup>T. Kikuchi, A. Watanabe, and K. Uchida, *Mater. Res. Bull.* **12**, 299 (1977).
- <sup>15</sup>R. E. Newnham, R. W. Wolfe, and J. F. Dorrian, *Mater. Res. Bull.* **6**, 1029 (1971).
- <sup>16</sup>J. V. Landuty, G. Remaut, and S. Amelinckx, *Mater. Res. Bull.* **4**, 329 (1969).
- <sup>17</sup>S. E. Cummins and L. E. Cross, *J. Appl. Phys.* **39**, 2268 (1968).
- <sup>18</sup>Y. Shimakawa, Y. Kubo, Y. Tauchi, H. Asano, T. Izumi, and Z. Hoiroi, *Appl. Phys. Lett.* **79**, 2791 (2001).
- <sup>19</sup>U. Chon, H. M. Jang, M. G. Kim, and C. H. Chang, *Phys. Rev. Lett.* **89**, 087601 (2002).
- <sup>20</sup>T. Watanabe, H. Funakubo, M. Osada, H. Uchida, and I. Okada, *J. Appl. Phys.* **98**, 024110 (2005).
- <sup>21</sup>S. Dunn, *J. Appl. Phys.* **94**, 5964 (2003).
- <sup>22</sup>H. Yan, F. Inam, G. Viola, H. Ning, H. Zhang, Q. Jiang, T. Zhang, Z. Gao, and M. J. Reece, *J. Adv. Dielectr.* **1**(1), 107 (2011).
- <sup>23</sup>G. Viola, T. Saunders, X. Wei, K. B. Chong, H. Luo, M. J. Reece, and H. Yan, *J. Adv. Dielectr.* **3**(1), 1350007 (2013).
- <sup>24</sup>A. Bell, in *Proceedings of the 9th International Symposium on Applied Ferroelectrics* (The Pennsylvania State University, University Park, PA, 1994), p.14.
- <sup>25</sup>P. Zheng, J. L. Zhang, Y. Q. Tan, and C. L. Wang, *Acta Mater.* **60**, 5022 (2012).
- <sup>26</sup>T. T. Chen, M. S. Fu, B. W. Jia, Y. J. Wu, X. Q. Liu, and X. M. Chen, *Adv. Appl. Ceram.* **112**, 270 (2013).
- <sup>27</sup>W. R. Buessem, L. E. Cross, and A. K. Goswami, *J. Am. Ceram. Soc.* **49**, 33 (1966).
- <sup>28</sup>G. A. Samara, *Phys. Rev.* **151**, 378 (1966).